FINAL-STATE INTERACTIONS OF RELATIVISTIC PROTONS

J. Ryckebusch, P. Lava and B. Van Overmeire[1, †]

[1] *Department of Subatomic- and Radiation Physics, Ghent University, Proeftuinstraat 86, B-9000 Gent, Belgium*
http://inwpent5.UGent.be/

At sufficiently large proton energies, Glauber multiple-scattering theory offers an economical way of describing the final state interactions in electro-induced proton emission off nuclear targets. A fully unfactorized and relativistic formulation of Glauber multiple-scattering theory is presented. Predictions are given for the separated ^{16}O$(e,e'p)$ response functions in quasi-elastic kinematics. The ^{16}O$(e,e'p)$ results are compared with data and the results of Relativistic Distorted-Wave Impulse Approximation calculations. Results for the nuclear transparencies in ^{12}C and ^{56}Fe are presented.

1. INTRODUCTION

From early in the seventies onward, exclusive $A(e,e'p)$ measurements, whereby the residual $A-1$ nucleus is left in the discrete part of its energy spectrum, have been extensively applied to study the low-energy part of the nuclear spectral function. The systematic measurements on various target nuclei revealed that the momentum distributions of bound protons in nuclei are in line with the predictions of the nuclear mean-field model. The occupation probabilities for the single-particle levels, on the other hand, turned out to be substantially smaller than what could be expected within the context of a naive mean-field model [1]. These findings provided sound evidence for the importance of short- and long-range correlations for the properties of nuclei [2].

From 1990 onward, the scope of $A(e,e'p)$ reactions has been widened. These days, rather than for studying mean-field properties, electro-induced single-proton knockout off nuclei is a tool to learn for example about relativistic effects in nuclei [3] or to study fundamental issues like possible medium modifications of protons and neutrons [4, 5]. Another timely issue is the question at what distance scales quark and gluons become relevant degrees of freedom for understanding the behavior of nuclei. Here, searches for the onset of the color transparency phenomenon in $A(e,e'p)$ reactions play a pivotal role [6]. In these studies one looks for departures from predictions for proton transparencies from models using standard nuclear-physics wave functions combined with the best available tools for describing final-state interactions (FSI).

Traditionally, the exclusive $A(e,e'p)$ measurements have been interpreted within the framework of the non-relativistic distorted wave impulse approximation (DWIA) [7, 8]. In the Impulse Approximation (IA), the electromagnetic interaction of the virtual photon with the target nucleus is assumed to occur through the individual nucleons. In the most simple DWIA versions, an independent particle model (IPM) picture is adopted and the initial and final A-nucleon wave functions are Slater determinants. The latter are composed of single-particle wave functions which are solutions to a one-body Schrödinger equation. Typically, in a DWIA approach the final proton scattering state is computed as an eigenfunction of an optical potential, containing a real and imaginary part. Parameterizations for these optical potentials are usually not gained from basic grounds, but require empirical input from elastic pA measurements. In the DWIA calculations, one adopts the philosophy that potentials which parameterize FSI effects in elastic $p + A \longrightarrow p + A$ reactions, can also be applied to model the proton's distortions in $A + e \longrightarrow A - 1 + e' + p$.

A research effort which started back in the late eighties has resulted in the development of a number of relativistic DWIA (RDWIA) models for computing $A(e,e'p)$ observables [10–14]. The available RDWIA frameworks adopt the independent-particle approximation with relativistic bound-state single-particle wave functions. They are customarily obtained from Hartree calculations within the context of the $\sigma - \omega$ model [15]. The scattering states, on the other hand, are solutions to a time-independent Dirac equation with relativistic optical potentials. Systematic surveys illustrated that in some $A(\vec{e},e'\vec{p})$ observables relativistic effects are sizable [16, 18] and that

[†] Electronic address: Jan.Ryckebusch@UGent.be

RDWIA-based calculations of $A(\vec{e},e'\vec{p})$ observables are at least as successful as the more traditional non-relativistic DWIA theories.

Given the highly inelastic character and diffractive nature of the proton-nucleon cross sections for proton lab momenta exceeding 1 GeV, the use of optical potentials for modeling FSI processes does not seem natural. In this energy regime, Glauber multiple-scattering theory provides an alternative and economical description of FSI mechanisms [19–21]. This model relies on the eikonal approximation and the assumption of consecutive cumulative scattering of a fast proton on a target composed of A-1 "frozen" scatterers. Most $A(e,e'p)$ calculations based on the Glauber approach are non-relativistic and/or factorized [22–26]. In Ref. [9] we have outlined a relativistic and unfactorized formulation of Glauber theory for calculating $A(e,e'p)$ observables. The major assumptions underlying our relativistic Glauber model bear a strong resemblance with those adopted in the RDWIA models developed during the last two decades. One of the pivotal assumptions underlying Glauber theory is the eikonal approximation.

The organization of this paper is as follows. First, in Sect. 2 we summarize the basic assumptions entering the relativized and unfactorized formulation of Glauber multiple-scattering theory. Section 3 is devoted to a discussion of some of the results obtained with the RMSGA framework. Section 4 summarizes our findings and states our conclusions.

2. RELATIVISTIC MULTIPLE-SCATTERING GLAUBER APPROXIMATION

The Relativistic formulation of the Multiple-Scattering Glauber approximation of Ref. [9] is based on the independent-nucleon framework and the Impulse Approximation (IA). This implies that the basic quantity to be evaluated when computing $A(\vec{e},e'\vec{p})$ observables is the following transition matrix element

$$\langle J^{\mu}\rangle = \int d\vec{r}\int d\vec{r}_2\ldots\int d\vec{r}_A \times\left(\Psi_A^{\vec{k}_p,m_s}\left(\vec{r},\vec{r}_2,\vec{r}_3,\ldots\vec{r}_A\right)\right)^{\dagger}\gamma^0 J^{\mu}(r)e^{i\vec{q}\cdot\vec{r}}\Psi_A^{gs}\left(\vec{r},\vec{r}_2,\vec{r}_3,\ldots\vec{r}_A\right), \quad (1)$$

where $\Psi_A^{\vec{k}_p,m_s}$ and Ψ_A^{gs} are the final and initial states which are modeled in terms of Slater determinants. Further, $J^{\mu}(r)$ is a one-body current operator.

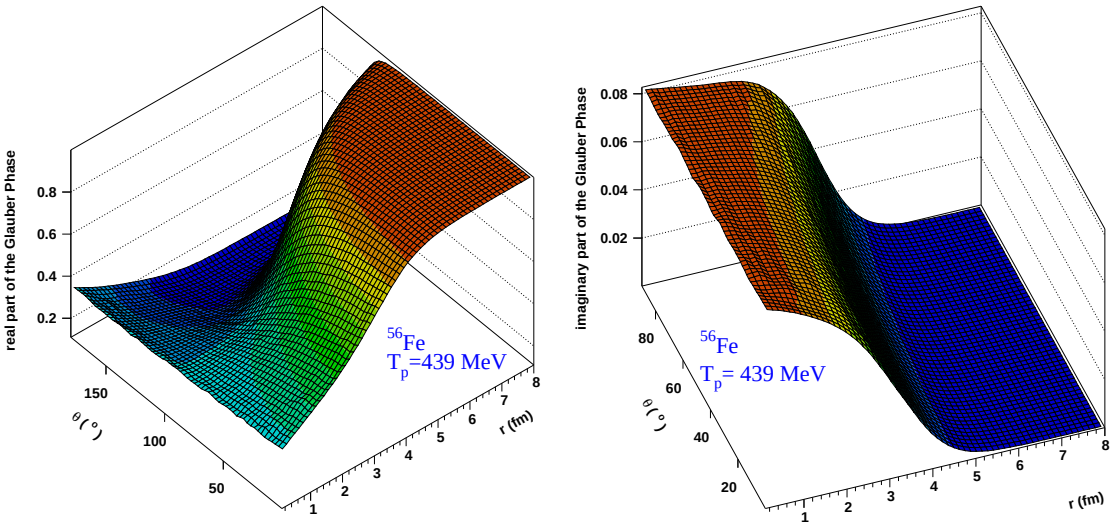

Fig. 1: The computed radial and polar-angle dependence of the real and imaginary part of the Dirac-Glauber phase for protons with T_p=439 MeV ejected from the Fermi level in ^{56}Fe.

The RMSGA framework adopts the eikonal approximation which is supposedly a valid one given the diffractive behavior of the elementary proton-nucleon scattering mechanisms at sufficiently large c.o.m. energies ($\sqrt{s}$) and small scattering angles (small $-t$). For the description of elastic $p-^{40}Ca$ processes, the Dirac eikonal approximation has been shown to be a valid one for kinetic energies $T_p \approx$500 MeV [27]. Adopting the eikonal approximation and assuming subsequent elastic rescattering from "frozen" spectator nucleons, the A-nucleon wave function in the final state of $e+A \longrightarrow e'+(A-1)+p$ reads

$$\Psi_A^{\vec{k}_p,m_s} = \mathcal{A}\Big[\widehat{\mathcal{S}}\left(\vec{r},\vec{r}_2,\dots\vec{r}_A\right)\left[\begin{array}{c}1\\ \frac{1}{E+M}\vec{\sigma}\cdot\vec{k}_p\end{array}\right]e^{\imath\vec{k}_p\cdot\vec{r}}\chi_{\frac{1}{2}m_s}\Psi_{A-1}^{J_R\,M_R}\left(\vec{r}_2,\vec{r}_3,\dots\vec{r}_A\right)\Big]\,, \tag{2}$$

where $\Psi_{A-1}^{J_R\,M_R}$ is the wave function describing the state in which the residual nucleus is created, $\mathcal{A}$ is the anti-symmetrization operator, and the A-body operator which accounts for all FSI mechanisms reads

$$\widehat{\mathcal{S}}\left(\vec{r},\vec{r}_2,\vec{r}_3,\dots\vec{r}_A\right) \equiv \prod_{j=2}^{A}\left[1-\Gamma\left(\vec{b}-\vec{b_j}\right)\theta\left(z_j-z\right)\right]. \tag{3}$$

Here, the product extends over all spectator nucleons. They act as possible scattering centers for the hit proton in its way out of the target nucleus. Very often, the above-mentioned A-body operator $\widehat{\mathcal{S}}$ is expanded according to

$$\begin{aligned}\widehat{\mathcal{S}}(\vec{r},\vec{r}_2,\vec{r}_3,\dots\vec{r}_A) \approx 1 &- \sum_{j=2}^{A}\theta(z_j-z)\Gamma(\vec{b}-\vec{b}_j)\\ &+\sum_{j\neq k=2}^{A}\theta(z_j-z)\Gamma(\vec{b}-\vec{b}_j)\theta(z_k-z)\Gamma(\vec{b}-\vec{b}_k)-\dots\,.\end{aligned} \tag{4}$$

In the expansion, the first term refers to "free passage" of the hit proton, the second to situations whereby it has been subject to "single scattering" mechanisms before leaving the target nucleus, and the third to "double scattering" processes. For a heavy nucleus like ^{208}Pb convergence of the above series is not reached until including quadruple-scattering terms [9]. In Eq. (3), the profile function Γ takes on the following form

$$\Gamma(k_p,\vec{b}) = \frac{\sigma_{pN}^{tot}(1-i\epsilon_{pN})}{4\pi(\beta_{pN})^2}\exp\left(-\frac{b^2}{2{\beta_{pN}}^2}\right)\,. \tag{5}$$

The profile function contains three parameters which depend on the proton kinetic energy. σ_{pN}^{tot} are the total pN cross sections, β_{pN} the so-called slope parameters and ϵ_{pN} the ratio of the real to imaginary part of the pN scattering amplitude. In our numerical calculations, we did not rely on the truncated operator of Eq. (4) but implemented the operator from Eq. (3) in its full complexity. This makes the numerical calculations increasingly involving as the mass number increases.

Eventually, within the RMSGA framework, the transition matrix element from Eq. (1) reduces to

$$\langle J^\mu\rangle = \int d\vec{r}\,\phi_{k_p m_s}^{\dagger}\left(\vec{r}\right)\mathcal{G}^{\dagger}(\vec{b},z)\gamma^0 J^\mu(\vec{r})e^{\imath\vec{q}\cdot\vec{r}}\phi_{\alpha_1}\left(\vec{r}\right)\,, \tag{6}$$

where $\phi_{\alpha_1}\left(\vec{r}\right)$ is the Dirac bound-state wave function obtained from the $\sigma-\omega$ model in the Hartree approximation, $\phi_{k_p m_s}^{\dagger}\left(\vec{r}\right)$ is a relativistic plane wave and $\mathcal{G}(\vec{b},z)$ the Dirac-Glauber phase which reads

$$\begin{aligned}\mathcal{G}(\vec{b},z) = \prod_{\alpha_{occ}\neq\alpha}\Bigg\{1 &- \frac{\sigma_{pN}^{tot}(1-i\epsilon_{pN})}{4\pi\beta_{pN}^2}\int_0^\infty b'db'\int_{-\infty}^{+\infty}dz'\theta(z'-z)\\ &\left(\left[\frac{G_{n\kappa}\left(r'(b',z')\right)}{r'(b',z')}\mathcal{Y}_{\kappa m}(\Omega',\vec{\sigma})\right]^2+\left[\frac{F_{n\kappa}\left(r'(b',z')\right)}{r'(b',z')}\mathcal{Y}_{\kappa m}(\Omega',\vec{\sigma})\right]^2\right)\\ &\times\exp\left[-\frac{(b-b')^2}{2\beta_{pN}^2}\right]\int_0^{2\pi}d\phi_{b'}\exp\left[\frac{-bb'}{\beta_{pN}^2}2\sin^2\left(\frac{\phi_b-\phi_{b'}}{2}\right)\right]\Bigg\}\,.\end{aligned} \tag{7}$$

The coordinate z' is chosen along the asymptotic direction of the ejectile. It is worth stressing that for the hit proton each nucleon in the residual $(A-1)$ nucleus acts as a "frozen" scattering center and is represented by its own relativistic single-particle wave function which has an upper $(G(r))$ and lower $(F(r))$ component. Cylindrical symmetry about the axis defined by the ejectile's asymptotic momentum makes the Dirac-Glauber phase to depend on two independent variables (b, z). Hereby, $b = \mid \vec{b} \mid$, where $\vec{b}$ is orthogonal to the ejectile's direction.

As an example, in Fig. 1 results are displayed for the computed real and imaginary part of the Glauber phase

$$\mathcal{G}(r,\theta) = \mathcal{G}\left(b = \sqrt{r^2 - r^2\cos^2\theta}\,, z = r\cos\theta)\right)\,, \tag{8}$$

corresponding with proton emission from the Fermi level in ^{56}Fe with $T_p = 439$ MeV. The θ denotes the polar angle with respect to the axis defined by the asymptotic momentum of the ejected particle. We remind that in the absence of final-state interactions the real part of the Glauber phase equals one, whereas the imaginary part vanishes identically. In the process of evaluating the ^{56}Fe$(e,e'p)$ matrix elements and performing the integrations over r and θ, the functions displayed in Fig. 1 quantify the FSI effects. The matrix elements are determined by the values of the Glauber phase folded with a relativistic bound-state wave function, a relativistic plane wave and a current operator. The radial coordinate "r" denotes the distance relative to the center of the target nucleus and the Glauber phase at this value gives a measure of the FSI mechanisms which the hit nucleon will undergo when the photon hits it at that position. For a given r, an additional non-trivial integration over the polar angles θ has to be performed. Here, $0^o \leq \theta \leq 90^o$ ($90^o \leq \theta \leq 180^o$) refers to a situation where the photon hits the nucleon in the forward (backward) hemisphere with respect to the direction defined by $\vec{k}_p$. The $\theta = 180^o$ case corresponds with a peculiar event whereby the photon couples to the proton along the direction defined by $-\vec{k}_p$. For $\theta = 180^o$ and increasing r, one considers the (rare) occasions that the photon hits the proton at the outskirts of the target nucleus at the opposite side of the detector and the proton has to travel through the whole target nucleus before it becomes asymptotically free. It speaks for itself that these kinematic situations induce the largest FSI effects but cannot be expected to provide large contributions to the integrated matrix elements as it usually refers to situations with extreme missing momenta.

3. RESULTS

First, we wish to compare the results of the $A(e,e'p)$ RMSGA calculations with alternate relativistic approaches to the same reaction. The RDWIA framework estimates the effect of FSI mechanisms by means of a radial-dependent complex optical potential. The parameterizations of these potentials are obtained from global fits to measured differential cross sections for elastic pA reactions [17]. It speaks for itself that the RDWIA approach emphasizes the proton-nucleus inelasticities as the major source of FSI mechanisms. The RMSGA framework, on the other hand, puts proton-nucleon inelasticities forward as the major source of FSI distortions and uses relativistic single-particle wave functions to describe the motion of the individual scattering centers in the residual $A-1$ nucleus. We have made a consistent comparison of the results from RMSGA and RDWIA calculations for the ^{16}O$(e,e'p)$ reaction in a kinematic regime where both approaches can be expected to be applicable. In comparing the predictions of the two models, all the ingredients apart from the description of the FSI effects, are kept identical. For example, for the comparisons shown in Fig. 2 both types of frameworks have used the same set of relativistic bound-state wave functions, dipole electromagnetic form factors, a CC2 current operator and the Coulomb gauge. The RDWIA curves of Fig. 2 are obtained with the Madrid implementation of the RDWIA framework [13]. We wish to stress that the RDWIA and RMSGA models adopt very different numerical techniques to compute the scattering wave functions and the corresponding matrix elements. The Madrid RDWIA code [13] employs a partial-wave expansion to solve the Dirac equation for the ejectile. The cylindrical symmetry of the Dirac-Glauber phase in Eq. (7) prevents any meaningful use of this technique in the RMSGA calculations. Instead, the multi-dimensional integrals are computed numerically. In the limit of vanishing FSI, however, the RDWIA-Madrid and RMSGA-Gent $A(e,e'p)$ codes should produce identical results when run with the same input parameters. In the RDWIA framework, the effect of FSI can be artificially made vanishing by nullifying the real and imaginary parts of the optical potentials when determining the scattering wave functions. In

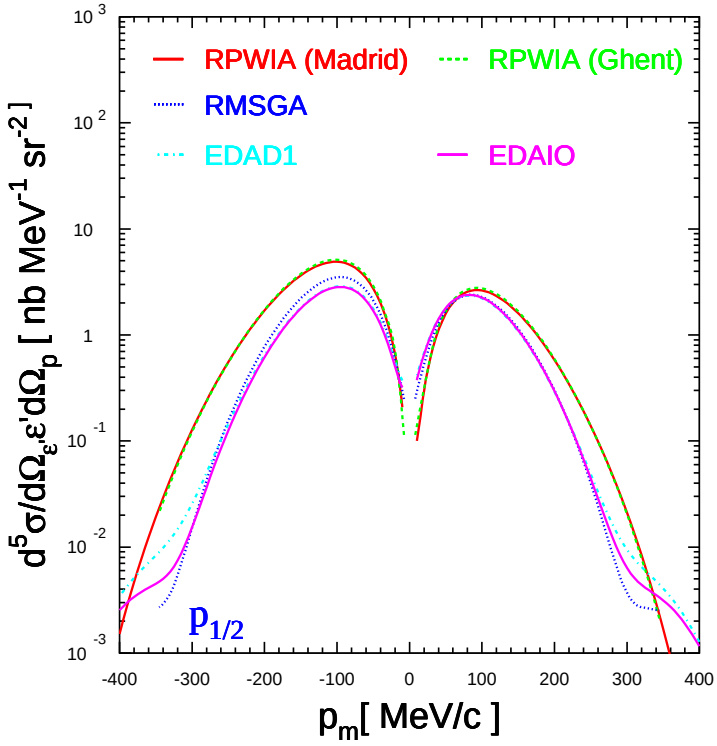

Fig. 2: The differential cross section versus missing momentum for proton knockout from the $1p_{1/2}$ orbit in ^{16}O$(e,e'p)$ at ω=0.439 GeV and Q^2=0.8 (GeV/c)^2 in constant (q,ω) kinematics. The various curves are explained in the text.

the RMSGA model, neglecting FSI mechanisms corresponds with putting $\mathcal{G}(b,z)=1$. As can be appreciated from Fig. 2, in the limit of vanishing FSI, which corresponds with the so-called Relativistic Plane-Wave Impulse Approximation (RPWIA), the RMSGA-Gent and RDWIA-Madrid codes produce differential cross sections with an agreement better than 5%. This lends support for the numerical methods used in both computer codes. The remaining differences are attributed to numerical errors. Remark that the Madrid code is conceived exact at the percent level as has been checked by comparing RPWIA results obtained through partial-wave expansions with the analytical expressions which exist in the limit of vanishing FSI. Figure 2 displays also the RDWIA predictions with two different parameterizations (EDAD1 and EDAIO) for the relativistic optical potentials along with the RMSGA result. The Glauber and optical-potential results are unexpectedly similar. The predicted reduction of the RPWIA cross section attributed to FSI mechanisms is comparable in both approaches. Furthermore, it appears that the eikonal approximation remains valid up to the highest missing momenta ($p_m \approx 350$ MeV/c) which have been considered in the numerical calculations. The RMSGA predicts a stronger asymmetry of the differential cross section between the positive and negative missing-momentum side, than the RDWIA model. This difference is likely due to the lack of a spin-orbit term in the Glauber-based approach.

Figure 3 compares the predictions of our unfactorized and relativistic Glauber calculation for the separated ^{16}O$(e,e'p)$ response functions with the data. Surprisingly, the 'out-of-the-box' and parameter-free Glauber calculations provide a reasonable description of these separated response functions for a proton kinetic energy of about 440 MeV.

Quasi-elastic $A(e,e'p)$ reactions have been performed to study the nuclear transparency as a function of the four-momentum transfer Q^2 and to look for the onset of signatures of the color-transparency phenomenon. The nuclear transparency provides a measure of the likelihood that a struck "nucleon" escapes from a target nucleus. The Q^2 and A dependence of this quantity is a

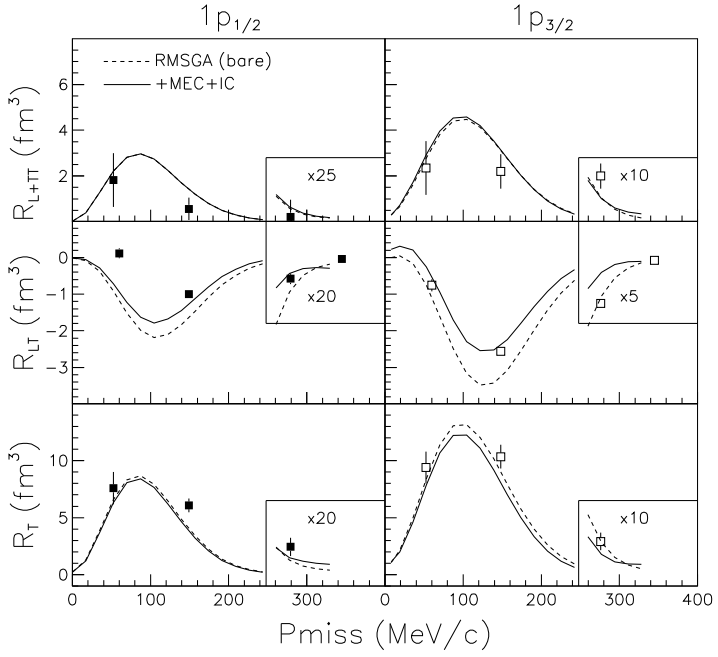

Fig. 3: Response functions for the removal of protons from the $1p$-shell in ^{16}O$(e,e'p)$ at ω=0.439 GeV and Q^2=0.8 (GeV/c)^2 in constant (q,ω) kinematics. The data are from Refs. [3, 28]. The dashed lines are obtained in the IA. The solid lines include also (non-relativistic) meson-exchange and isobar currents. The adopted spectroscopic factors are 0.6 ($1p_{1/2}$) and 0.7 ($1p_{3/2}$).

possible source of information about the onset of the color transparency phenomenon and the (non-hadronic) small-size components in the nucleon. The transparency is extracted from the measured $A(e,e'p)$ differential cross sections by means of

$$T = \frac{\int_{\Delta^3 k} d\vec{k} \int_{\Delta E} dE\ S_{exp}(\vec{k},E)}{c_A \int_{\Delta^3 k} d\vec{k} \int_{\Delta E} dE\ S_{NRPWIA}(\vec{k},E)}\ ,$$

with the reduced cross section S_{exp} determined by

$$S_{exp}(\vec{k}=\vec{k}_f-\vec{q}, E=\omega-T_p) = \frac{\frac{d^5\sigma}{d\Omega_p de' d\Omega_{e'}}(e,e'p)}{K\sigma_{ep}^{CC1}}$$

The integration over $\Delta^3 k$ and ΔE in the above formulae refers to kinematic ranges in the missing momentum and energy for which the impulse approximation is believed to be valid. In practice, this is achieved by setting the upper limits $p_m \leq k_F$ (with k_F the Fermi momentum) and $E_m \leq 80$ MeV. Our results for the nuclear transparencies in ^{12}C and ^{56}Fe are summarized in Fig. 4. Whereas the Carbon data are reasonably well described, the calculations systematically underpredict the measured transparencies for Iron. The trends of the calculations are not dramatically different from what is found in typical non-relativistic Glauber approaches. The theoretical curves in Fig. 4 are obtained by summing the computed differential cross section for all occupied single-particle states in constant (q,ω) kinematics. Thereby, we consider analogous kinematic ranges for the missing momentum and energy as in the experiments. For each of the occupied single-particle states the Glauber phase was computed. We did not address the kinematic range below Q^2=0.6 (GeV/c)^2 given the limits imposed by the eikonal approximation.

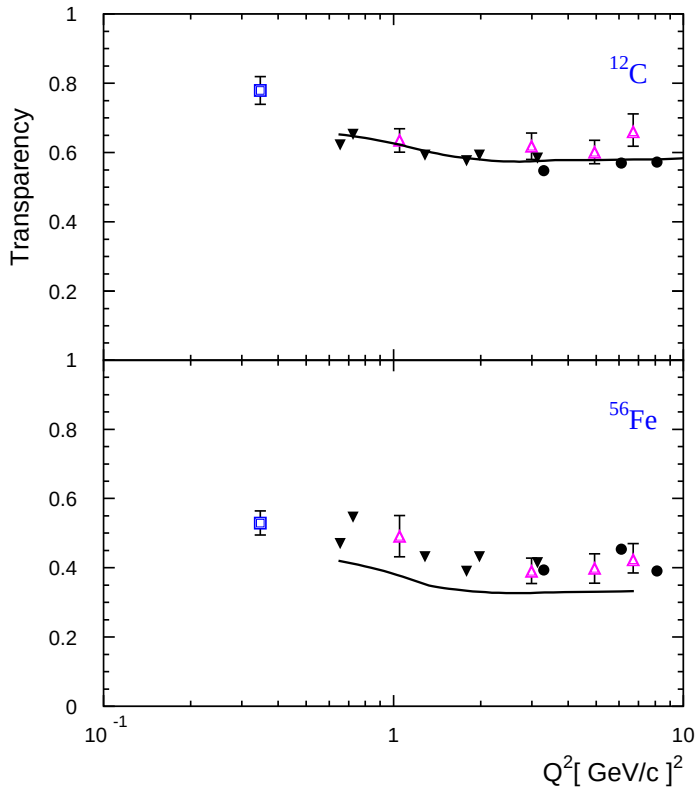

Fig. 4: Nuclear transparencies versus Q^2 for $A(e,e'p)$ reactions in quasi-elastic kinematics. Data are from Refs. [29] (open squares), [30, 31] (open triangles), [32] (solid circles) and [33, 34] (solid triangles).

4. CONCLUSIONS

A fully unfactorized and relativized formulation of Glauber multiple-scattering theory for modeling exclusive $A(e,e'p)$ processes is presented. Compared to the RDWIA models, the relativistic Glauber approximation holds stronger links with the elementary proton-proton and proton-neutron processes and does not require the (phenomenological) input of optical potentials based on fits to elastic pA data. Our fully unfactorized framework can accommodate most of the relativistic effects which are usually implemented in the RDWIA approaches. Like in the RDWIA models, the bound-state wave functions are solutions to a Dirac equation with scalar and vector potentials fitted to the ground-state nuclear properties, i.e. an approach commonly known as the $\sigma - \omega$ model.

The relativized Glauber multiple-scattering formalism can be applied to calculate $A(\vec{e},e'\vec{p})$ observables for any even-even target nucleus starting from ^{4}He. We wish to stress that Glauber approaches appear in very different flavors. Our framework avoids many of the approximations, like the factorization assumption or the introduction of a thickness function, which are commonly adopted in literature.

We find that the relativistic RMSGA differential cross sections follow similar trends than the RDWIA ones. This observation points towards a smooth transition between the typical low- and high-energy regime for describing final-state interactions [35]. Despite the very different philosophies underlying an optical-potential and Glauber approach, their predictions for the $A(e,e'p)$ observables are not that dramatically different. The relativistic Glauber approach provides a fair description of the measured nuclear transparencies. In our formulation of the Glauber framework, though, it emerges that also unintegrated quantities like response functions and polarizations observables can be reliably computed.

Acknowledgements
We wish to thank M.C. Martínez and J.M. Udías for providing the RDWIA calculations and numerous discussions.

REFERENCES

[1] V. Pandharipande, I. Sick, P. deWitt Huberts, Rev. Mod. Phys. 69 (1997) 981.
[2] H. Müther, A. Polls, Prog. Part. Nucl. Phys. 45 (2000) 243.
[3] J. Gao et al., Phys. Rev. Lett. 84 (2000) 3265.
[4] S. Malov et al., Phys. Rev. C 62 (2000) 057302.
[5] S. Dieterich et al., Phys. Lett. B 500 (2001) 47.
[6] K. Garrow et al., Phys. Rev. C 66 (2002) 044613.
[7] S. Boffi, C. Giusti, F. Pacati, Phys. Rep. 226 (1993) 1.
[8] J. Kelly, Adv. Nucl. Phys 23 (1996) 75.
[9] J. Ryckebusch, D. Debruyne, P. Lava, S. Janssen, B. Van Overmeire and T. Van Cauteren, Nucl. Phys. A 728 (2003) 226.
[10] A. Picklesimer, J. Van Orden, S. Wallace, Phys. Rev. C 32 (1985) 1312.
[11] J. Johansson, H. Sherif, G. Lotz, Nucl. Phys. A 605 (1996) 517.
[12] Y. Yin, D. Onley, L. Wright, Phys. Rev. C 45 (1992) 1311.
[13] J. Udias, P. Sarriguren, E. Moya de Guerra, E. Garrido, J. Caballero, Phys. Rev. C 48 (1993) 2731.
[14] A. Meucci, C. Giusti, F. Pacati, Phys. Rev. C 64 (2000) 64014605.
[15] B. Serot, J. Walecka, Adv. Nucl. Phys. 16 (1986) 1.
[16] J. Udias, J. Vignote, Phys. Rev. C 62 (2000) 034302.
[17] E. Cooper, S. Hama, B. Clarck, R. Mercer, Phys. Rev. C 47 (1993) 297.
[18] M. Martínez, J. Caballero, T. Donnelly, Nucl. Phys. A 707 (2002) 83.
[19] R. Glauber, G. Matthiae, Nucl. Phys. B 21 (1970) 135.
[20] S. J. Wallace, Phys. Rev. C 12 (1975) 179.
[21] D. Yennie, Interaction of high-energy photons with nuclei as a test of vector-meson-dominance, in: J. Cummings, D. Osborn (Eds.), Hadronic Interactions of Electrons and Photons, Academic, New York, 1971, p. 321.
[22] O. Benhar, N. Nikolaev, J. Speth, A. Usmani, B. Zakharov, Nucl. Phys. A 673 (2000) 241.
[23] C. Ciofi degli Atti, L. Kaptari, D. Treleani, Phys. Rev. C 63 (2001) 044601.
[24] S. Jeschonnek, T. Donnelly, Phys. Rev. C 59 (1999) 2676.
[25] A. Kohama, K. Yazaki, R. Seki, Nucl. Phys. A 662 (2000) 175.
[26] L. Frankfurt, M. Strikman, M. Zhalov, Phys. Lett. B 503 (2001) 73.
[27] R. Amado, J. Piekarewicz, D. Sparrow, J. McNeil, Phys. Rev. C 28 (1983) 1663.
[28] K.G. Fissum and the Hall-A collaboration, in preparation.
[29] G. Garino et al., Phys. Rev. C 45 (1992) 780.
[30] T. O'Neill et al., Phys. Lett. B 351 (1995) 87.
[31] N. Makins et al., Phys. Rev. Lett. 72 (1994) 1986.
[32] K. Garrow et al., Phys. Rev. C 66 (2002) 044613.
[33] D. Abbott et al., Phys. Rev. Lett. 80 (1998) 5072.
[34] D. Dutta, preprint nucl-ex/0303011 (2003).
[35] D. Debruyne, J. Ryckebusch, S. Janssen and T. Van Cauteren, Phys. Lett. B 527 (2002) 62.